Hydromagnetic flow and heat transfer of a micropolar fluid over an exponentially stretching sheet through a porous medium with slip effects

E. O. Fatunmbi[1*], A. Adeniyan[2]

[1] Department of Mathematics and Statistics, Federal Polytechnic, Ilaro, Nigeria
[2] Department of Mathematics, University of Lagos, Akoka, Lagos, Nigeria.
E-mail: [1]ephesus.fatunmbi@federalpolyilaro.edu.ng, [2]aadeniyan@unilag.edu.ng
Corresponding author: [1]ephesus.fatunmbi@federalpolyilaro.edu.ng

Abstract

The flow of hydromagnetic dissipative micropolar fluid passing an exponentially stretching two-dimensional vertical sheet influenced by buoyancy force, radiation and slip effects is examined in this study. The dimensional modelled equations of the flow have been translated from partial into ordinary differential equations via similarity conversion approach while the solution to the transmuted equations is found using shooting technique alongside fourth order Runge-Kutta scheme. A strong relationship exists between the current results and the related published ones in literature for limiting situations. Various graphs have been sketched to discuss the impact of the key parameters as related to the fields of velocity, temperature and microrotation while tables are used to identify and explain the influences of some of the controlling parameters on the coefficient of the skin friction and Nusselt number for both Newtonian and non-Newtonian micropolar fluids. It is noticed that the growth of velocity slip lowers the fluid motion while the thermal slip behaves the same manner on the temperature field.

Keywords: Buoyancy force, hydromagnetic, micropolar fluid, exponentially stretching sheet

1. INTRODUCTION

Micropolar fluid concept initiated and extended to thermo-micropolar fluid by Eringen [1-2] has offered an interesting research area for researchers and scientists in the recent years owing to its practical usefulness as related to science, technology and industrial operations]3]. Each particle of such fluids is made of different sizes such that each has the tendency to vary in shapes, either to shrink, expand and rotate separately from the rotational movement of the fluid [4]. This concept has been found suitable for modeling flow of various complex fluids such as suspension solution, animal blood, liquid crystals, polymeric fluids etc. [5]. Some areas of applications include: polymer engineering, drug suspension in pharmacology, sediments in rivers, biological fluid modeling, crude oil extraction, food processing manufacturing and many others. These fluids are also found applicable in diverse areas of bio-engineering sciences such as synovial lubrication, arterial blood flows, knee cap mechanics, cervical flows, pharmacodynamics etc. [6].

Hydromagnetic flow in porous medium becomes important in various scientific aplications such as in geothermal energy extractions, ground water hydrology, MHD generators, etc. In view of these applications, researchers have paid more attention to such study on different

goemetries, boundary conditions engaging various types of fluids [7-10]. At high operating temperatures, the influence of thermal radiation becomes germane, this occurs due to the emission from the heated wall and the working fluid. In various engineering operations, such as in gas turbines, astrophysical flows, power plants, etc, the understnding of thermal radiation becomes crucial, for instance, in polymer extrusion works, the quality of the output during fabrication processes is determined to some extent on thermal controlling factors, hence, the desired product can be optimally achieved with the intended characteristics when there is accurate knowledge of radiation heat transfer [11-14].

The aforementioned researches were however conducted with the concept of no-slip condition at the wall. However, it has been observed that this assumption fails in some practical situations and in such cases, the partial slip at the wall may readily be invoked. This becomes crucial in situations where the flow pressure is small or the flow system is characterized by small size as well as when investigating particulate fluids such as emulsions and polymer solutions. This type of study is also applicable in biomedical engineering, science and technology as reported in [15-19].

The investigation of flow prompted by a stretching sheet offers a practical usefulness in numerous engineering and industrial operations. In particular, in metallurgical operations, including the cooling of continuous strips or filaments drawn through a quiescent fluid, the strips are commonly stretched, and in such cases, the value of the end product is determined by the rate of stretching as well as cooling rate. By drawing such strips in a micropolar fluid which is electrically conducting due to magnetic field influence ensures that the rate of cooling can be decided such that the grade of the desired output can be better achieved. As a pioneer on such study, Crane [20] provided a similarity solution in closed analytical nature on a two-dimensional sheet which streches linearly such that the velocity and the distance from the silt are proportional to each other. Various investigators have improved on such study by adding different parameters, geometries and wall conditions [21-23]. However, low attention has been given to the study involving nonlinear and/or exponential stretching of plastic sheet in literature. This kind of problem is commonly encountered in practical cases such as in annealing and thinning of copper wire. Hence, the need to investigate such problem. Exponentially stretching sheet flow and heat transfer properties of Newtonian fluids have been reported by various scholars [24-28] with non-similar solution whereas Adeniyan and Adigun [29] provided a pure similarity solution on such problem only with assumption of no-slip condition and without employing non-Newonian micropolar fluid inspite of its huge practical applications.

Taking cognizance of the enormous applications of this type of study in various areas of science an engineering as highligted above, the current work is therefore undertaken to extend the work of Adeniyan and Adigun [29] by making use of non-Newtonian microplar fluid as the working fluid as against the Newtonian fluid engaged by those researchers and by incoporating slip condition effects at the boundary as against the no-slip assumption applied by [29]. The model developed in this study is numerically solved while the influences of some chosen parameters have been investigated on the skin friction coeffient and Nusselt number for the non-Newtonian micropolar fluid and compared with Newtonian fluid.

2 Problem Formulation and Governing Equations

The flow Hydromagnetic micropolar fluid passing an inclined vertical, exponentially stretching two-dimensional sheet in porous medium as sketched in Figure 1 is considered. The problem investigated in this study goes with the assumption that the flow is steady and characterized by viscous dissipation, heat generation, radiation and Joule heating with effects of Navier slip at the boundary. As depicted in Figure 1, the coordinate system is similarly assumed to be (x, y) having the corresponding components of velocity as (u, v). In addition, the flow is assumed to be in x direction while y-axis is perpendicular to it, the external magnetic field of uniform strength B_0 is applied perpendicular to the flow direction whereas the induced magnetic field is negligible in comparison to the external magnetic field. The flow is also confined to the region $y > 0$. The fluid velocity is $u = U_w + U_{sl}$where U_w and U_{sl} are the sheet and slip velocity respectively. The temperature of the fluid is $T = T_w + \delta \frac{\partial T}{\partial y}$ where T_w is the sheet temperature and δ is the thermal slip factor.

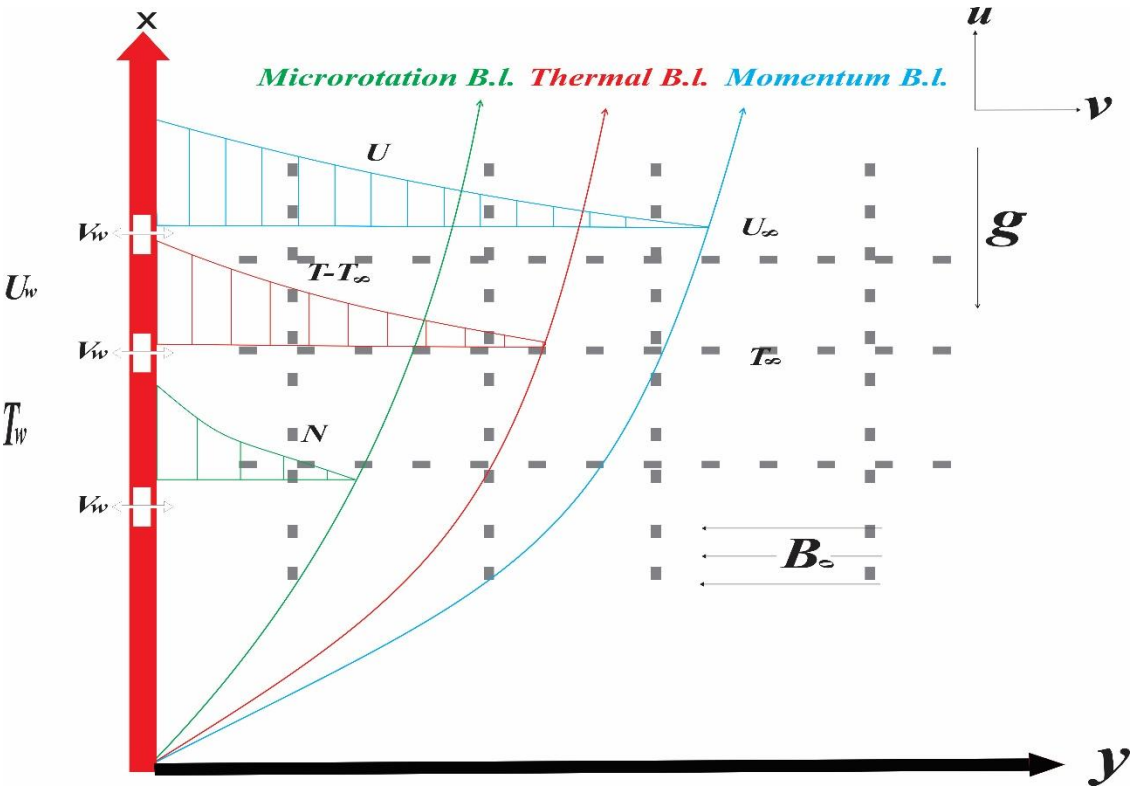

Fig. 1: The Physical Flow Geometry

Using the above described assumptions, Oberbeck-Boussinesq together with the usual boundary layer approximations, the modelled equations can be listed as:

$$\frac{\partial u}{\partial x} + \frac{\partial v}{\partial y} = 0 \tag{1}$$

$$u\frac{\partial u}{\partial x}+v\frac{\partial u}{\partial y}=\frac{(\mu+r)}{\rho}\frac{\partial^2 u}{\partial y^2}+\frac{r}{\rho}\frac{\partial N}{\partial y}+g\beta_0(T-T_\infty)-\frac{\sigma B_0^2}{\rho}u-\frac{\mu}{\rho K_p}u \tag{2}$$

$$\rho j\left(u\frac{\partial N}{\partial x}+v\frac{\partial N}{\partial y}\right)=\gamma\frac{\partial^2 N}{\partial y^2}-r\left(2N+\frac{\partial u}{\partial y}\right) \tag{3}$$

$$u\frac{\partial T}{\partial x}+v\frac{\partial T}{\partial y}=\frac{k}{\rho Cp}\frac{\partial^2 T}{\partial y^2}-\frac{1}{\rho Cp}\frac{\partial q_r}{\partial y}+\frac{(\mu+r)}{\rho Cp}\left(\frac{\partial u}{\partial y}\right)^2+\frac{\mu}{\rho C_p K_p}u^2+\frac{\sigma B_0^2}{\rho Cp}u^2+\frac{Q}{\rho C_p}(T-T_\infty). \tag{4}$$

The appropriate boundary conditions are stated as:

$$y=0:\ u=U_w+\zeta\frac{\partial u}{\partial y},\ v=V_w,\ N=-n\frac{\partial u}{\partial y},\ T=T_w+\delta\frac{\partial T}{\partial y} \tag{5}$$

$$y\to\infty:\ u\longrightarrow 0,\ N\longrightarrow 0,\ T\longrightarrow 0.$$

In Eqs. (1-5), u and v are velocity components given in x and y directions respectively, ν denotes kinematic viscosity whereas T represents fluid temperature. Also, $u_w=U_0e^{\left(\frac{x}{L}\right)}$, $T_w=T_\infty+T_0e^{\left(\frac{2x}{L}\right)}$, U_0, T_0 and L are the stretching velocity, sheet temperature, a constant having the unit of speed for the stretching sheet, reference constant temperature and reference length respectively and T_∞ is the free stream temperature. Following Seini and Makinde [27], $\sigma=\sigma_0e^{\left(\frac{x}{L}\right)}$ is the electrical conductivity while N is a symbol showing microrotation component whereas $K_p=K_0e^{\left(\frac{x}{L}\right)}$ describes the porous medium permeability, $V_w=V_0e^{\left(\frac{x}{2L}\right)}$, *is the* suction/injection ($V_w<0$ is suction, ($V_w>0$ is injection), while ρ stands for the fluid density, C_p indicates the specific heat at constant pressure, k symbolizes thermal conductivity, B_0 is the constant magnetic field strength. Also, $\zeta=\alpha_1e^{-\left(\frac{x}{2L}\right)}$ implies the velocity slip, $\delta=\beta_1e^{-\left(\frac{x}{2L}\right)}$ is the thermal slip factor [30], μ stands for the dynamic viscosity while r indicates vortex or microrotation viscosity, Q= $Q_0e^{\left(\frac{x}{L}\right)}$ is the heat source/sink, $j=j_0e^{-(x/L)}$ denotes micro-inertia density and $j_0=\frac{\nu L}{U_0}$, γ is the spin gradient viscosity, β_0 indicates thermal expansion coefficient while σ_0, Q_0, K_0 and V_0 are constants, Also, n is the microrotation parameter at the boundary with $0\le n\le 1$ [31-33]. We remark also that when $r=0$, the velocity and microrotaion are decoupled. Similarly, on setting $\gamma=\kappa=j=0$, the set of Eqs. (1-4) reduces to that of Newtonian fluids.

Various researchers including, Adeniyan [34] as well as Akinbobola and Okoya [35] have shown that the radiative heat flux q_r can have the structure givenin (6). By assuming small temperature diffrence within the flow, T^4 can thus be expressed as a linear combination of the temperature and it can be expanded by Taylor series about T_∞^4. Neglecting higher order terms ands taking the derivative, Eq. (6) becomes (7).

$$\mathrm{q_r}=-\frac{4\sigma^*}{3\alpha^*}\frac{\partial T^4}{\partial y} \tag{6}$$

$$\frac{\partial q_r}{\partial y} = -\frac{16\sigma^\star T_\infty^3}{3\alpha^\star}\frac{\partial^2 T}{\partial y^2} \tag{7}$$

In Eqs. (6-7) $\sigma^\star \; and \; \alpha^\star$ represent Stefan Boltzmann constant and mean absorption coefficient in that order. With the use of the stream function (8) it is evident that Eq. (1) is valid,

$$u = \frac{\partial \psi}{\partial y}, \;\; \nu - \frac{\partial \psi}{\partial x}. \tag{8}$$

Also, Eqs. (2-5) have been translated from partial to ordinary differential equations by introducing Eq. (9) see [17, 19],

$$\psi = (2\nu L U_0)^{\frac{1}{2}} e^{\left(\frac{x}{2L}\right)} f(\eta), \;\; \eta = y\left(\frac{U_0}{2\nu L}\right)^{\frac{1}{2}} e^{\left(\frac{x}{2L}\right)},$$
$$N = \left(\frac{U_0^3}{2\nu L}\right)^{\frac{1}{2}} e^{\left(\frac{3x}{2L}\right)}, \; T = T_\infty + T_0 e^{\left(\frac{2x}{L}\right)}\theta(\eta). \tag{9}$$

Substituting Eq. (9) into Eqs. (2--5) and using (8) gives nonlinear ODEs as:

$$(1+K)f''' + ff'' - 2f'^2 + Kg' + Gr\theta - H_D f' = 0 \tag{10}$$

$$\lambda g'' + fg' - 3f'g - 2KH(2g + f'') = 0 \tag{11}$$

$$\left(1 + \frac{4}{3}R\right)\theta'' + \Pr(f\theta' - 4\theta f' + Q\theta) + PrEc\, f''^2 + PrEcH_D f'^2 = 0. \tag{12}$$

The boundary conditions become

$$\eta = 0: f' = 1 + \alpha f'', \;\; f = fw, \qquad g = -nf'', \theta = 1 + \beta\theta,$$
$$\eta \longrightarrow \infty: \; f' = 0, \; g \longrightarrow 0, \; \theta \longrightarrow 0. \tag{13}$$

Here, the differentiation is carried out with respect to η. The material (micropolar) parameter is represented by $K = r/\mu$ and the microrotation density parameter is symbolized as $\lambda = \frac{\gamma}{\mu j}$. Also $\alpha = \alpha_1\left(\frac{U_0}{2\nu L}\right)^{\frac{1}{2}}$ indicates the velocity slip term while $\beta = \beta_1\left(\frac{U_0}{2\nu L}\right)^{\frac{1}{2}}$ is the thermal slip term, $H_D = 2\left[\frac{\sigma_0 B_0^2 L}{\rho U_0} + \frac{\mu L}{\rho U_0 K_0}\right]$ describes the Hartmann-Darcy term (accounting for the combined impact of the magnetic field and the homogeneous porous medium permeability), $fw = -V_0\left(\frac{2L}{U_0\nu}\right)^{\frac{1}{2}}$ describes suction/injection parameter ($fw > 0$ suction while $fw < 0$ injection, $Pr = \frac{\mu\, C_p}{k}$ is the Prandtl number whereas the term indicating heat source/sink is symbolized as $Q = 2Q_0 \, \mathrm{L}/\rho U_0 C_p$, $Ec = \frac{U_0^2}{C_p T_0}$ stands for Eckert number, $R = (4\sigma^\star T_\infty^3)/\alpha^\star k$ is the radiation parameter, $H = \frac{\nu L}{U_0 j_0}$ denotes vortex viscosity parameter and $Gr = (2g\beta_0 T_0 L)/U_0^2$ is the Grashof number.

Eq. (14) describes the related quantities of engineering interest which are the skin friction, Nusselt number and the wall couple stress coefficient given as:

$$C_{fx} = \frac{\tau_w}{\rho u_w^2},\ Nu_x = \frac{Lq_w}{k(T_w - T_\infty)},\ M_w = \left(\gamma \frac{\partial N}{\partial y}\right) \tag{14}$$

where

$$\tau_w = \left[(\mu + r)\partial u/\partial y\ + rN\right]_{y=0},\ q_w = -k\left[\frac{\partial T}{\partial y}\right]_{y=0} \tag{15}$$

The first term in Eq. (15) describes the wall shear stress whereas the second term respresents the surface heat flux. With the use of Eq. (9) and Eq. (15), the quantities in (14) respectively become

$$C_{fx}^{\star} = f''(0), N^{\star}u_x = -\theta(0),\ C^{\star}s = g'(0), \tag{16}$$

where

$$C_{fx}^{\star} = \frac{\frac{1}{\sqrt{2}}(Re_x)^{\frac{1}{2}}}{(1+(1-nK))}C_{fx}, N^{\star}u_x = -\sqrt{2}(Re_x)^{-\frac{1}{2}}Nu_x,\ C^{\star}s = 2\nu LM_w/\gamma u_w^2$$

are the skin friction coeffient, Nusselt number, wall couple stress coerffient in that order and the local Reynolds number is $Re_x = \frac{u_w L}{\nu}$.

3 Numerical Solution

The transmuted set of Eqs. (11-13) is a boundary value problem which are first translated converted into a system of first order ordinaty differential equations.We assume that

$$f_1 = f, f_2 = f', f_3 = f'', f_4 = g, f_5 = g', f_6 = \theta, f_7 = \theta',\ \tag{17}$$

$$f_3' = \frac{2f_2'^2 - f_1 f_3\ - Kf_5 - Grf_6 + H_D f_2}{(1+K)} \tag{18}$$

$$f_5' = \frac{3f_2 f_4 + 2KH(2f_4 + f_3) - f_1 f_5}{\lambda} \tag{19}$$

$$f_7' = \frac{-Pr(f_1 f_7 - 4f_6 f_2 + Q\ \ f_6 + Ecf_3^2 + EcH_D f_2^2)}{\left(1 + \frac{4}{3}R\right)} \tag{20}$$

The boundary conditions translate to

$$\begin{gathered} f_1(0) = fw, f_2(0) = 1 + \alpha f_3, f_3(0) = p_1, f_4(0) = -nf_3(0),\ f_5(0) = p_2 \\ f_6(0) = 1 + \beta f_7,\ f_7(0) = p_3,\ \ f_2(\infty) \longrightarrow 0, f_4(\infty) \longrightarrow 0,\ \ f_6(\infty) \longrightarrow 0 \end{gathered} \tag{21}$$

The unspecified initial conditions $p_1 = f''(0),\ p_2 = g'(0)$, and $p_3 = \theta'(0)$ have been determined by applying the shooting technique. After obtaining $p_1,\ p_2$ and p_3 then we have employed fourth-order Runge-Kutta technique with step size $\nabla\eta = 0.01$ and the solution is obtained with a tolerance limit of 10^{-7}.

4 Results Analysis and Discussion

For effective discussion of the results generated in the current work, the numerical computations are analyzed both with the constructed graphs and tables. The analysis has been carried out for the following controlling parameters: material (micropolar) parameter K, velocity slip parameter α, thermal slip parameter β, microrotation density parameter λ, vortex viscosity parameter H, Hartmann-Darcy parameter H_D, Prandtl number Pr, radiation parameter R, suction/injection parameter fw, Eckert number $Ec\ and$ heat source (or sink) parameter Q. We have made use of the underlisted values for the controlling parameters: $K = Gr = \lambda = H_D, \beta = 1.0, \alpha = 0.3,\ R = Ec = 0.1, fw = 0.5, Q = 0.2, n = 0.5,\ Pr = 0.71$. Unless otherwise mentioned on the plots.
In the absence of the microrotation equation (Eq. 2), the material (micropolar) parameter K, the velocity and thermal slips parameters, the problem in this work reduces to that of [29]. For the sake of validation with existing results of Bidin & Nazar [36] and Mukhopadhyay [30] we have replaced the coefficient "4" in the term $\theta f'$ in Eq. (13) by "1" . This does not affect the authencity of the present result. The numerical scheme is thus verified by comparing the computed values of $N^{\star}u_x$with the existing works of [36], [30] and [29] for some limiting situations with variations in Pr. It is evident from Table 1 that a strong relationship exists among the comparisons.

Table 1

Computed values of $N^{\star}u_x$ for variation in Pr and R when $H_D, K, \alpha, \beta, Ec, H, Q, R = fw = 0$

Pr	***R***	**Bidin & Nazar [36]**	**Mukhopadhyay [30]**	**Adeniyan & Adigun [29]**	**Present Results**
1.0	0	0.9547	0.9547	0.95485201	0.9548106
3.0		1.8691	1.8691	1.869061724	1.8690688
5.0		-	2.5001	2.500122587	2.5001280
10.0		-	3.6603	3.660365072	3.6603693
1.0	1.0	0.5315	0.5311	0.537337859	0.5353012
2.0		1.0735	1.0734	-	1.0735162
3.0	0.5	1.3807	1.3807	-	1.3807451

Furthermore, comparison of $C_{fx}^{\star}$ and $N^{\star}u_x$ obtained in this work for variation in R and Ec agrees well with that of Seini and Makinde [27] for some limiting situations as depicted in Table 2.

Table 3 displays the computed values of $C_{fx}^{\star}$and $N^{\star}u_x$ for micropolar and Newtonian fluids for changes in the values of the Hartmann-Darcy parameter H_D, velocity slip parameter α, thermal slip parameter β and Eckert number Ec. It is conspicuously noticed from this table that the

values of $C_{fx}^{\star}$ for a micropolar fluid are lower than the corresponding values of the Newtonian fluid with an increase in H_D, α, β and Ec.

Table 2

Computed values of $C_{fx}^{\star}$ and $N^{\star}u_x$with [27] for $R\ and\ Ec$ with $Pr = 0.71$ while $H_D, K, Ec, \alpha, \beta, fw, Q, R = 0$

		Seini & Makinde [27]		Present Results	
R	Ec	$C_{fx}^{\star}$	$N^{\star}u_x$	$C_{fx}^{\star}$	$N^{\star}u_x$
0.0	1.0	1.629178	-0.006337	1.6291778	-0.0063379
0.1	1.0	1.629178	0.006964	1.6291778	0.0069647
0.5	1.0	1.629178	0.035754	1.6291778	0.0357547
0.1	2.0	1.629178	-0.598521	1.6291778	-0.5985207
0.1	3.0	1.629178	-1.204006	1.6291778	-1.2040062

Table 3

Values of $C_{fx}^{\star}$ and $N^{\star}u_x$ for variations in H_D, α, β and Ec.

				Micropolar Fluid		**Newtonian Fluid**	
H_D	α	β	Ec	$C_{fx}^{\star}$	$N^{\star}u_x$	$C_{fx}^{\star}$	$N^{\star}u_x$
0.0	0.3	1.0	0.1	0.5973747	0.5864942	0.8197306	0.5610731
1.0				0.7414607	0.5584511	0.9946504	0.5266762
3.0				0.9381281	0.5137339	1.2247594	0.4726876
5.0				1.0765975	0.4766906	1.3797858	0.4298266
1.0	0.1			0.9330780	0.5710755	1.3684405	0.5436416
	0.5			0.4395287	0.5281715	0.5177767	0.4951253
	1.5			0.3423427	0.5144845	0.3872402	0.4838322
	3.0			0.2068135	0.4907360	0.2210951	0.4672901
	0.3	0.1		0.6808540	1.1913225	0.8958823	1.0882682
		0.5		0.7414607	0.5584511	0.9946504	0.5266762
		1.5		0.7544545	0.4325054	1.0177197	0.4116810
		3.0		0.7730773	0.2584982	1.0528155	0.2499576
		1.0	0.05	0.7437231	0.5664145	0.9969028	0.5320998
			0.3	0.7325316	0.5269921	0.9857161	0.5051342
			0.6	0.7194555	0.4808902	0.9725144	0.4732391
			1.0	0.7025064	0.4212080	0.9552154	0.4313896

This clearly shows that fluids characterized by microstructures and additives suspensions tend to lower the viscous drag as compared to Newtonian fluid. To be more specific, as the velocity slip parameter α rises from 0.1 to 3.0, the rate of decrease in $C_{fx}^{\star}$is 78% for the micropolar fluid whereas the corresponding decrease is 83% for the Newtonian fluid. Also, for the Newtonian fluid, the

rate of increase in $C_{fx}^{\star}$ is 68% whereas that of micropolar fluid is 80% while the rate of heat transfer reduces by 23% for the Newtonian fluid with corresponding reduction of 19% for the micropolar fluid as H_D rises from 0 to 5.0. Moreover, observation clearly indicates that the values of $N^{\star}u_x$ indicating the heat transfer at the sheet surface for the Newtonian fluid are lower than the corresponding values of the micropolar fluid with an increase in H_D, α, β and Ec. Specifically, $N^{\star}u_x$ for the micropolar fluid reduces by 78% (or 14%) when β ($or\ \alpha$) increases from 0.1 to 3 whereas this reduction is 77% (or 13%) in the Newtonian fluid. The rate of heat transfer also drops by 26% for the Newtonian fluid as Ec increases from 0.05 to 1.0 whereas this drop is only 10% in the micropolar fluid.

Table 4 illustrates the influences of parameters K, Pr, R, fw, Gr and λ on $C_{fx}^{\star}$, $N^{\star}u_x$ and $C^{\star}s$. From this table, it is observed that $C_{fx}^{\star}$as well as $C^{\star}s$ decreases with growing values of the material (micropolar) parameter K, radiation parameter R, injection parameter $fw < 0$, Grashof number Gr and the microrotation density parameter λ whereas $C_{fx}^{\star}$ grows with Pr and fw. Meanwhile, the parameters $K, Pr\ , fw > 0, Gr$ and λ enhance $N^{\star}u_x$ while the parameters $R, fw < 0$ reduces rate of heat transfer. These results indicate that the presence of micro-particles tends to reduce the drag effect while enhancing heat transfer rate.

Table 4

Values of $C_{fx}^{\star}, N^{\star}u_x$ and $C^{\star}s$ for variations in K, Pr, R, fw, Gr and λ

K	Pr	R	fw	Gr	λ	$C_{fx}^{\star}$	$N^{\star}u_x$	$C^{\star}s$
0.0	071	0.1	1.0	1.0	1.0	0.9946504	0.5266762	0.7687710
1.5						0.6677167	0.5668222	0.4659584
3.0						0.5247803	0.5811103	0.3100913
	1.0					0.7567499	0.6083422	0.5589718
	1.5					0.7711788	0.6636942	0.5693515
	2.5					0.7840882	0.7259503	0.5801830
		0.2				0.7359532	0.5418519	0.5460749
		0.4				0.7260094	0.5131326	0.5404235
		1.0				0.7028073	0.4503678	0.5279026
			-1.0			0.5590127	0.4883861	0.2820376
			-0.4			0.6240388	0.5149280	0.3648757
			0.4			0.7272081	0.5533926	0.5243001
			1.0			0.8167923	0.5843312	0.6955248
				0.0		0.8099592	0.5466010	0.6077389
				2.0		0.6806244	0.5667388	0.4932359
				5.0		0.5215765	0.5835472	0.3336177
					0.1	0.7361091	0.5595564	0.3992181
					2.0	0.7325289	0.5604010	0.3327680
					3.0	0.7276194	0.5616717	0.2652037

Figures 2-4 portray the behaviour of K on the dimensionless velocity, temperature and microrotation fields respectively. It is conspicuously seen that the velocity appreciates with a corresponding increase in the momentum boundary layer thickness with growth in K.

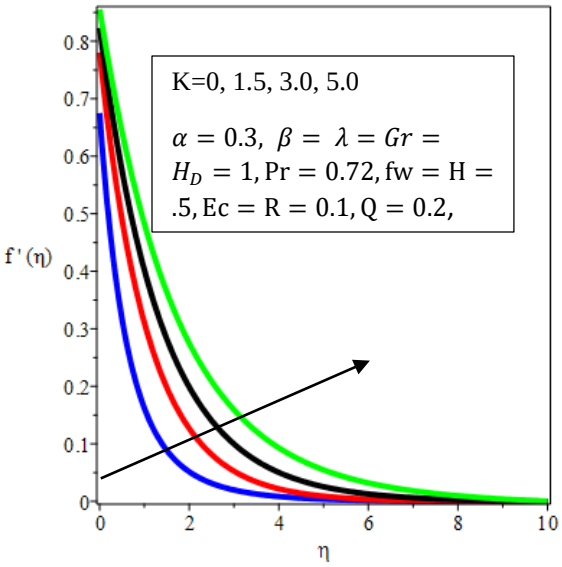

Fig. 2. Variation of K on Velocity profile

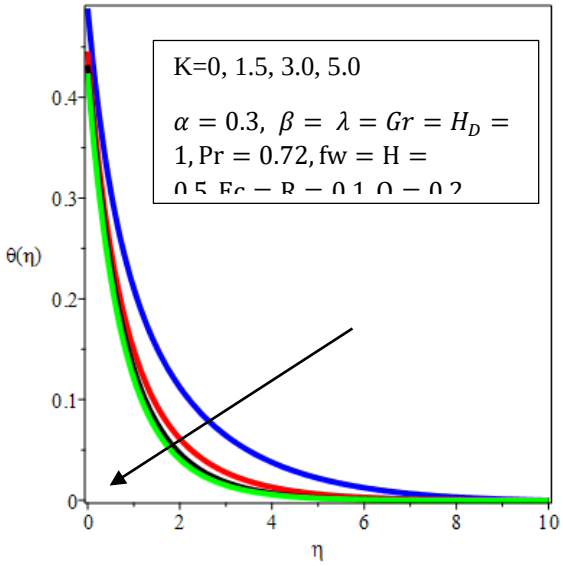

Fig. 3. Impact of K on Temperature field

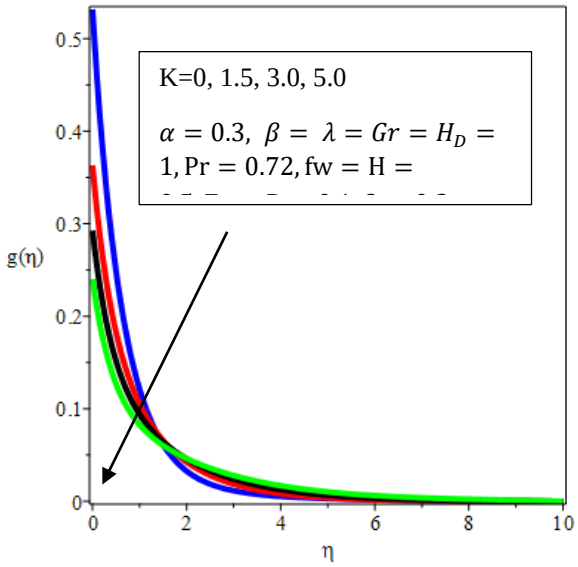

Fig. 4. Microrotation field for K

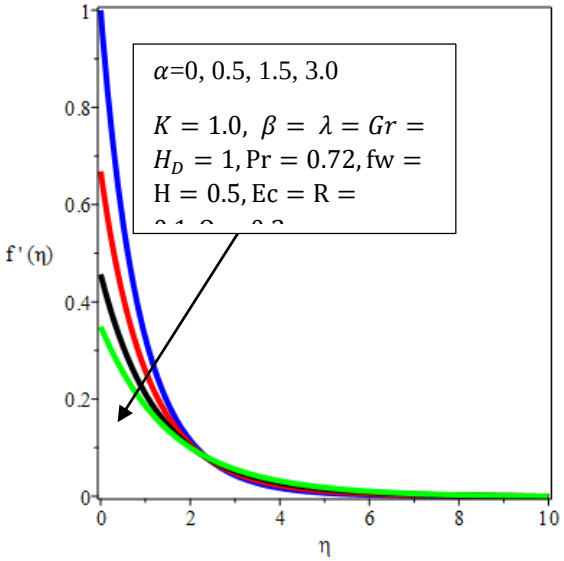

Fig. 5. Velocity profiles for α

The increase in the magnitude of K causes a reduction in the drag (see Table 4) which in turn facilitates the fluid motion as shown in Figure 2. Conversely, the thermal and microrotation

boundary layers become thin with rising values of K. This in turn leads to a decline in the temperature and microrotation distributions across as displayed in Figures 3 and 4.

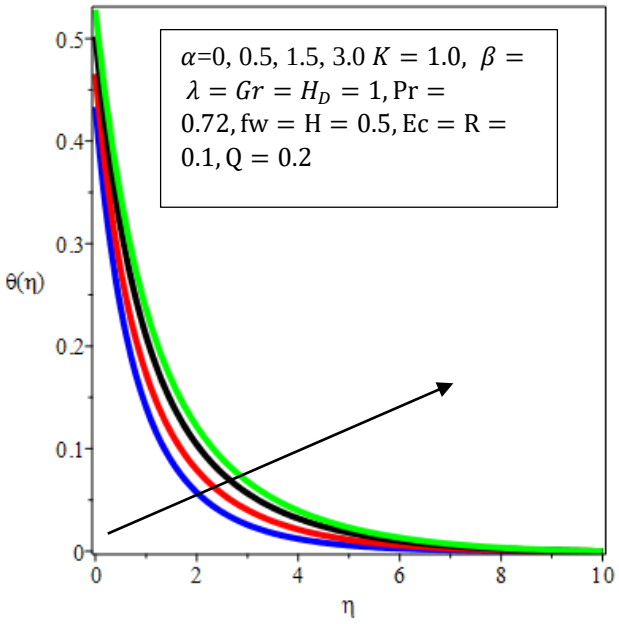

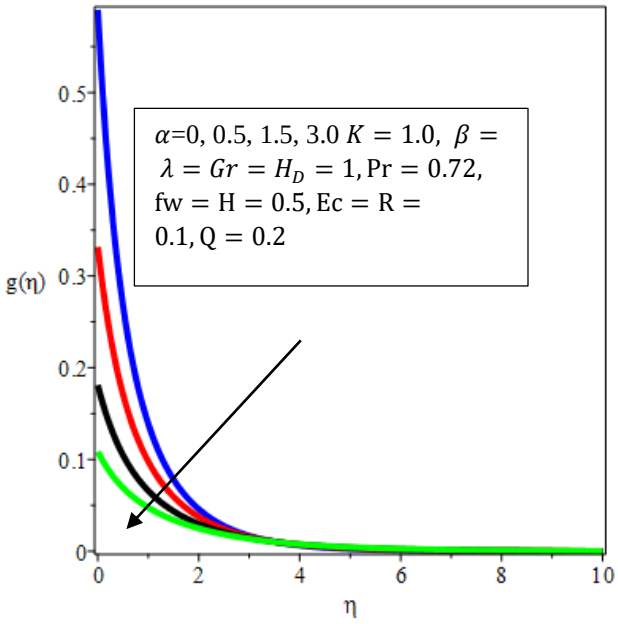

Fig. 6. Impact of α on Temperature

Fig. 7. Variation of α on Microrotation

The impact of velocity slip parameter α on the velocity, temperature and microrotation fields is showcased in Figures 5-7. It is seen that growing values of α tends to lower the velocity. This is so because the momentum generated by the stretching sheet is partly transmitted to the micropolar fluid in the presence of velocity-slip, hence a reduction in the fluid flow as depicted in Figure 5. Besides, an increase in the tightness of the porous medium occurs with a rise in H_D since it is a combination of both magnetic field and porous mediums. It is also an indication that the permeability stabilizes the boundary layer growth. Based on the resistance imposed on the fluid

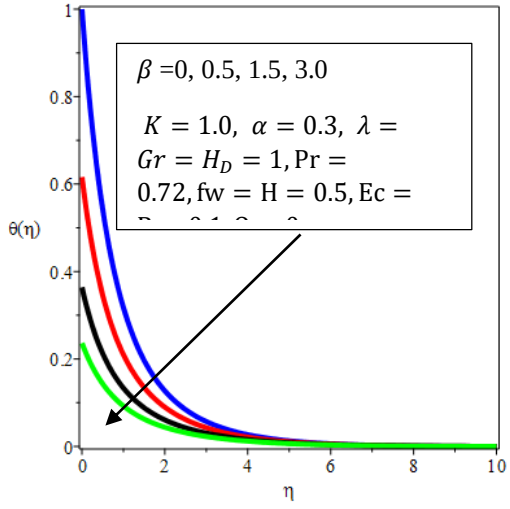

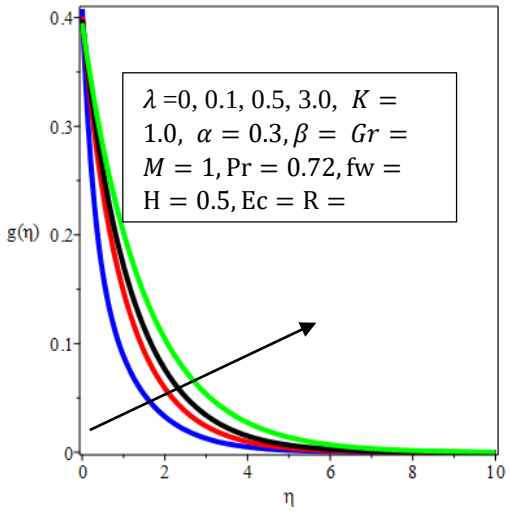

Fig. 8. Effect of β on Temperature

Fig. 9. Effect of λ on Microrotation

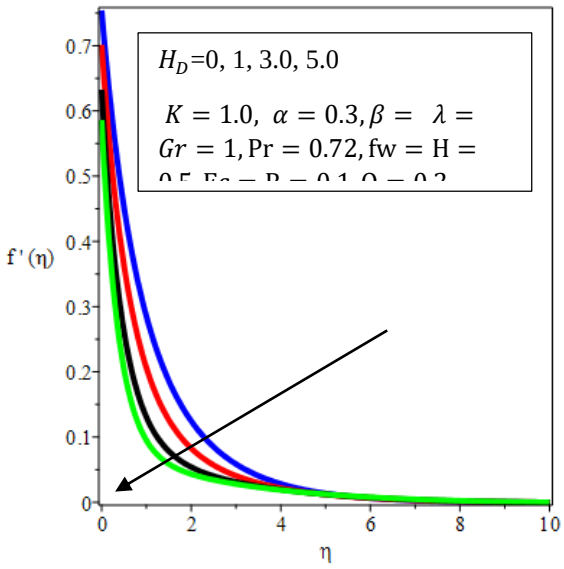

Fig. 10. Variation of H_D on Velocity profiles

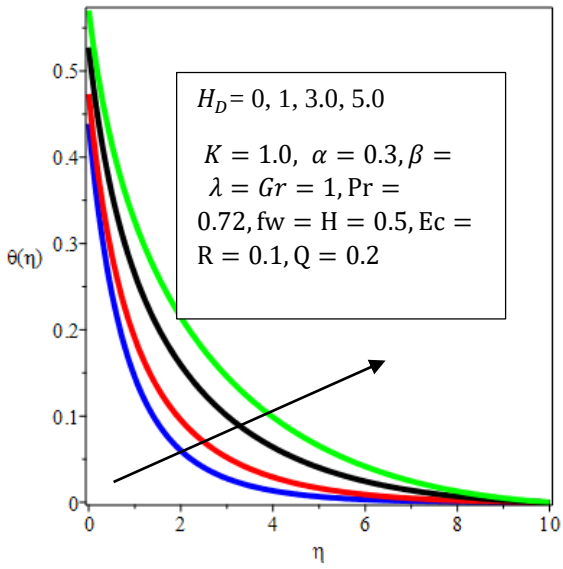

Fig. 11. Temperature profiles for H_D

Figure 6 indicates that the temperature profile is advancing as the magnitude of the slip parameter α grows. The response of the microrotation field to changes in α follows that of velocity profiles as illustrated in Figure 7. It is revealed in Figure 8 that rising values of the term β indicating thermal slip parameter β creates a reduction in the temperature distribution as well as lowering the thermal boundary thickness.

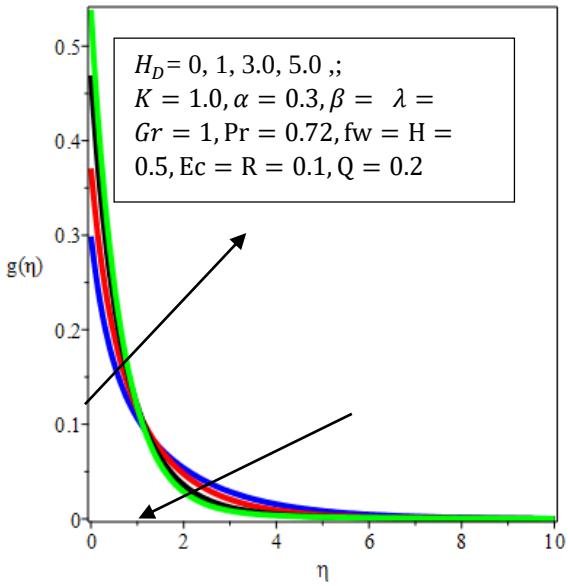

Fig. 12. Microrotation profiles for H_D

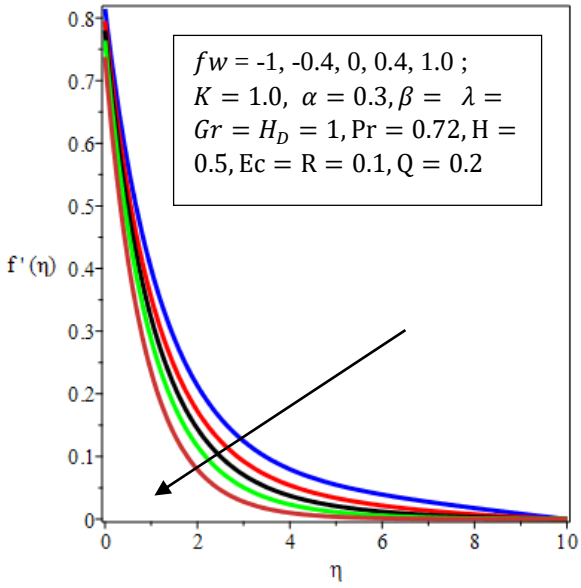

Fig. 13. Variation of fw on velocity field

The impact of microrotation density parameter λ on the microrotation profiles is exhibited in Figure 9, in this figure, the microrotation field is seen to advance in the presence of the micro-particles. Figures 10-12 show the combined influence of the magnetic and homogeneous porous

medium permeability parameter known as Hartmann-Darcy parameter H_D on the dimensionless quantities. Clearly, the fluid motion falls as H_D rises as noted in Figure 10. This can be linked to the imposition of the transverse magnetic field since the fluid is electrically conducting, the magnetic field creates a retarding force called Lorentz force which act to reduce the fluid flow.

Besides, an increase in the tightness of the porous medium occurs with a rise in H_D since it is a combination of both magnetic field and Darcy term. It is also an indication that the permeability stabilizes the boundary layer growth. Based on the resistance imposed to the fluid motion by Lorentz and Darcy forces, a rise in the temperature profiles is noticed with growing values of H_D as plotted in Figure 11.

Figure 12 explains that rising values of H_D facilitates the growth of microrotation field near the exponentially stretching sheet but away from the sheet the opposite trend is noticed. Figures 13-14 depict the responses of fw as respectively relates to velocity and thermal fields. Both velocity and temperature profiles depreciate as ($fw > 0$) advances in magnitude. That is, rising values of $fw > 0$ indicating suction have a lowering effect on both dimensionless quantities. This is due to the fact that as the heated micropolar fluid is being pushed towards the sheet, there is a resistance by the buoyancy force on the account of high viscosity. Conversely, the imposition of wall fluid injection $fw < 0$ creates a reverse trend.
The plot of temperature profiles against η for changes in Ec is sketched in Figure 15. Here, it is clear that rising values of Ec enhances the thermal boundary layer and in turn boost the temperature distribution because as Ec rises more heat is generated due to drag between the fluid particles.

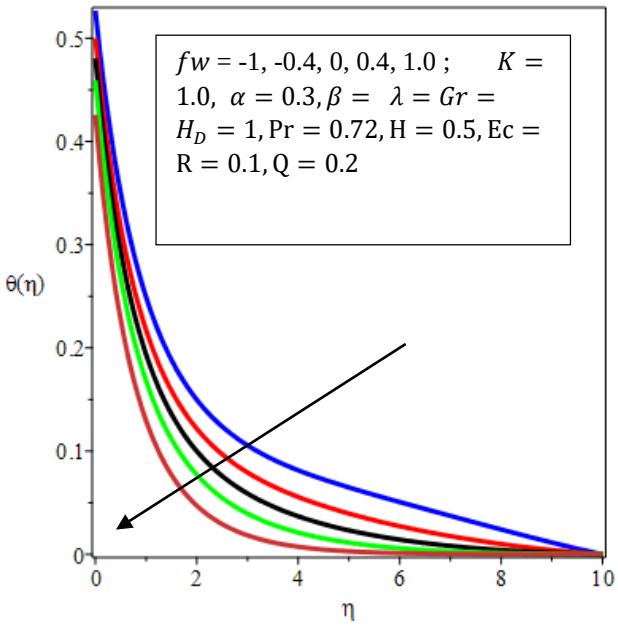

Fig. 14. Effect of fw on Temperature

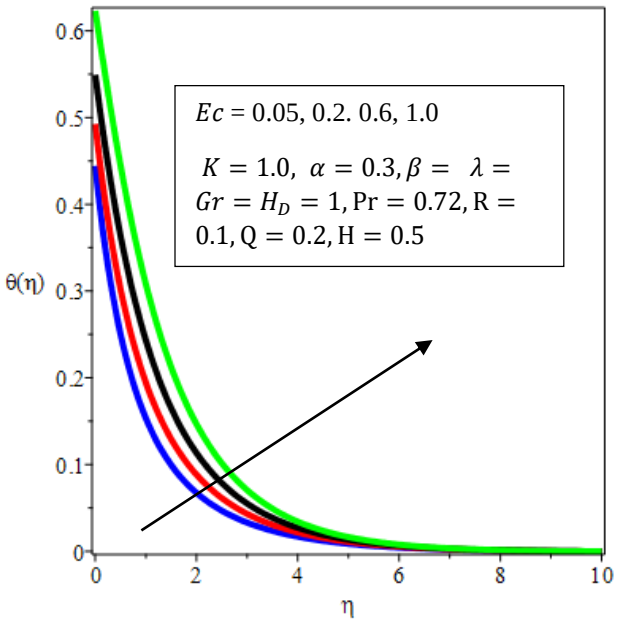

Fig. 15. Effect of Ec on Temperature profiles

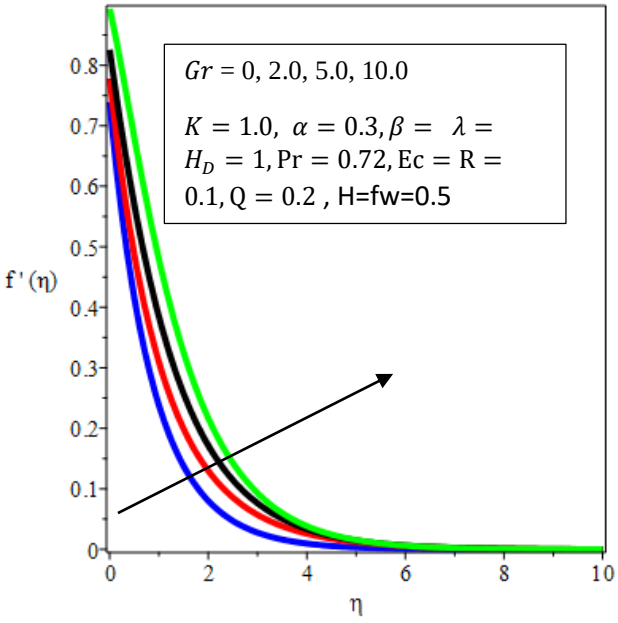

Fig. 16. Variation of Gr on Velocity field

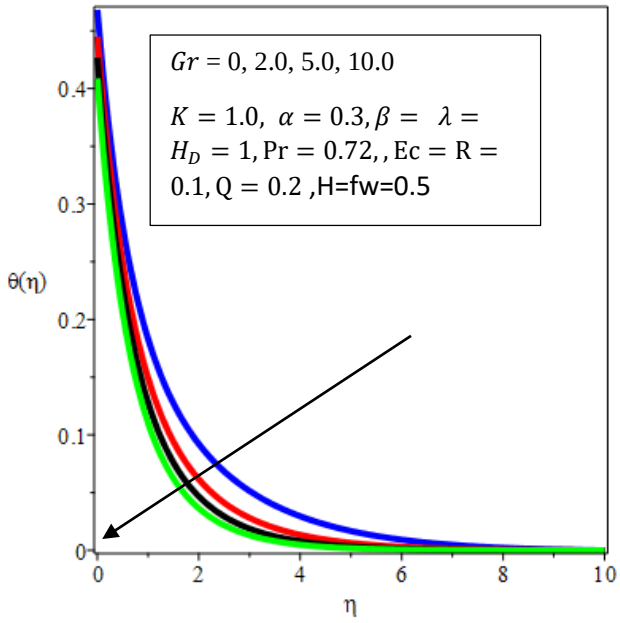

Fig. 17. Impact of Gr on Temperature

Figures 16-17 are the plots portraying the impact of the Grashof number on the profiles of both velocity and temperature. In Figure 16, the velocity increases as the magnitude of Gr rises because the motion of the fluid is enhanced by the buoyancy forces corresponding to an increase in Gr, the buoyancy forces act as a favourable pressure gradient advancing the fluid motion whereas the temperature profiles reduce as the magnitude of Gr increases as shown in Figure 17.

5. Conclusion

Hydromagnetic flow and heat transfer of an incompressible dissipative micropolar fluid over an exponentially stretching vertical sheet in a saturated porous medium has been investigated. The flow is influenced by both velocity and thermal slips. The system of equations governing the fluid flow and heat transfer has been numerically solved via shooting technique cum fourth order Runge-Kutta algorithms. The impacts of various controlling parameters have been examined by means of graphs as well as tables. From this study we note that:

- The momentum as well as microrotation boundary layer thickness reduces with an increase in the velocity slip parameter α while the thermal boundary layer thickens with a rise in α but falls with growing values of thermal slip parameter β.
- The values of C_{fx} for a Newtonian fluid are higher than the corresponding values of the micropolar fluid for the parameters $H_D.\alpha, \beta, Ec$. The implication of this is that, the use of micropolar fluid reduces the frictional drag along the sheet better than the Newtonian fluid.
- The rate of heat transfer for the Newtonian fluid is lower than that of the micropolar fluid for the embedded controlling parameters.
- An increase in the magnitude of the velocity slip parameter causes a reduction in both C_{fx} and Nu_x. Conversely, C_{fx} increases while Nu_x drops as the thermal slip β increases.

References

[1] Eringen, A. C. "Theory of micropolar fluids". *J. Math. Anal. Appl.*, 16 (1966): 1-18.

[2] Eringen, A. C. "Theory of thermo-microfluids". *Journal of Mathematical Analysis and Applications*, 38 (1072): 480-496.

[3] Rana1, B.M.J., Arifuzzaman, S. M., Reza-E-Rabbi, Sk., Ahmed, S. F., Khan, Md. "Energy and magnetic flow analysis of Williamson micropolar Nanofluid through stretching sheet". *International Journal of Heat and Technology***,** 37(2) (2019): 487-496. doi.org/10.18280/ijht.370215

[4] Lukaszewicz, G. *Micropolar fluids: Theory and Applications*, 1st Ed., (1999) Birkhauser, Boston.

[5] Chen, J., Liang, C. and Lee J. D. "Theory and simulation of micropolar fluid dynamics", J. *Nanoengineering and Nanosystems*, 224, 31-39 (2011).

[6] Reena, Rana, U. S. "Effect of Dust Particles on rotating micropolar fluid heated from below saturating a porous medium". *Applications and Applied Mathematics, An International Journal*, 4 (2009): 189-217.

[7] Olajuwon, B. I., Oahimire, J. I., Waheed, M.A. "Convection heat and mass transfer in a hydromagnetic flow of a micropolar fluid over a porous medium". *Theoret. Appl. Mech*. 41 (2014): 93-117.

[8] Fatunmbi, E. O and Fenuga, O. J. "MHD micropolar fluid flow over a permeable stretching sheet in the presence of variable viscosity and thermal conductivity with Soret and Dufour effects". *International Journal of Mathematical Analysis and Optimization: Theory and Applications*, (2017): 211- 232.

[9] Kareem, R. A. and Salawu, S. O. Islam, Md. R., Khan, Md. S. (2018). "Variable viscosity and thermal conductivity of Soret and Dufour on inclined magnetic field in non-Darcy permeable medium with dissipation". *British Journal of Mathematics & Computer Science*, 22(3) (2017), 1-12.

[10] Kasim, A. R. M., Arifin, N. S. Zokri, S. M and Salleh, M. Z. "Fluid particles interaction with buoyancy forces on Jeffrey fluid with Newtonian heating". *CFD Letters*, (2019): 1-16.

[11] Ibrahim, S. M., Suneetha, K. "Radiation and heat generation effects on steady MHD flow near a stagnation point on a linear stretching sheet in porous medium in presence of variable thermal conductivity and mass transfer". *Int. J Current Res. Aca.*, Rev 2(7) (2014): 89-100.

[12] Olanrewaju, P. O., Okedayo, G. T., Gbadeyan, J. A. "Effects of thermal radiation on magnetohydrodynamic (MHD) flow of a micropolar fluid towards a stagnation point on a

vertical plate". *International Journal of Applied Science and Technology*, 1(6) (2014): 1-12.

[13] Darbhashayanam, S., Mendu, U. "Thermal radiation and chemical reaction effects on magnetohydrodynamic free convection heat and mass transfer in a micropolar fluid". *Turkish Journal of Engineering and Environmental Sciences*, 38 (2014): 184-196

[14] Reddy, M. G. "Influence of Magnetohydrodynamic and thermal radiation boundary Layer Flow of a Nanofluid past a stretching sheet". *J. Sci. Res*. 6 (2) (2014): 257-272. http://dx.doi.org/10.3329/jsr.v6i2.17233

[15] Anderson, H. I. "Slip flow past a stretching surface". *Acta Mechanica*, 158 (2002): 121-125.

[16] Devi, R. L., Neeraja, A., Reddy, N. B. "Radiation effect on MHD slip flow past a stretching sheet with variable viscosity and heat source/sink, Int". *J. Sci and Innovative Mathematical Res*, 3 (2015): 8-17.

[17] Nandeppanavar, M. M., Vajravelu, K., Abel, M., Siddalingappa, M. N. "MHD flow and heat transfer over a stretching surface with variable thermal conductivity and partial slip, Meccanica", 48 (2013): 1451-1464.

[18] Das, K.: "Slip effects on heat and mass transfer in MHD micropolar fluid flow over an inclined plate with thermal radiation and chemical reaction". *Int. J. Numer. Meth. Fluids*, doi:10.2002/fd.2683

[19] Salawu, S.O, Oderinu, R. O.and Ohaegbue, A. D., "Thermal runaway and thermodynamic second law of a reactive couple stress hydromagnetic fluid with variable properties and Navier slips", *Scientific African*, (2019) doi: https://doi.org/10.1016/j.sciaf.2019.e00261

[20] Crane, L. J. "Flow past a stretching plate", *Communicatios Breves*, 21 (1970): 645-647.

[21] Salawu, S. O and Okedoye, A. M. "Effect of nonlinear radiative heat and mass flow over a stretching surface with variable conductivity and viscosity". *Journal of the Serbian Society for Computational Mechanics*, 13(2) (2019), 87-104

[22] Eldabe, N. T., Elshehawey, E. F., Elbarbary, M. E., Elgazery, N. S. "Chebyshev finite difference method for MHD flow of a micropolar fluid past a stretching sheet with heat transfer". *Journal of Applied Mathematics and Computation*, 160 (2001), 437-450.

[23] Reddy, M. G. "Heat generation and thermal radiation effects over a stretching sheet in a micropolar fluid". *International Scholarly Research Networks*, ,2012: 1-6. doi.org. /10.5402/2012/795814

[24] Magyari, E and Keller, B. "Heat and mass transfer in the boundary layers on an exponentially stretching continuous surface". *Journal of Physics*, 32 (1999): 577-585.

[25] El-Aziz, M. "Viscous dissipation effect on mixed convection flow of a micropolar fluid over an exponentially stretching sheet". *Can. J. Phy*, 87 (2009):359-368

[26] Mandal, I., Mukhopadhyay, S. "Heat transfer analysis for fluid flow over an exponentially stretching porous sheet with surface heat flux". *Ain Shams Eng. Journal*, (2013): 103-110.

[27] Seini, Y. I., Makinde, O. D. "MHD boundary layer flow due to exponentially stretching surface with radiation and chemical reaction". *Mathematical Problem in Engineering*, (2013): 1-7.

[28] Srinivasacharya, D. and RamReddy, Ch. "Soret and Dufour effects on mixed convection from an exponentially stretching surface". *Int. J. of Nonlinear Sci*. 12 (2011)**:** 60-68.

[29] Adeniyan, A., Adigun, J. A. "Similarity solution of hydromagnetic flow and heat transfer past an exponentially stretching permeable vertical sheet with viscous dissipation, Joulean and viscous heating effects". *Annals of Faculty Engineering Hunedoara-International Journal of Engineering*, (2016): 1-8.

[30] Mukhopadhyay, S. "Slip effects on MHD boundary layer flow over an exponentially stretching sheet with suction/blowing and thermal radiation". *Ain Shams Engineering Journal*, (2013): 485-491.

[31] Ahmadi, G. "Self-similar solution of incompressible micropolar boundary layer flow over a semi-infinite plate". *Int. J. Engng Sci*, 14 (1976): 639-646. Sciences, 5:700-710.

[32] Jena, S. K. and Mathur, M. N. "Similarity solutions for laminar free convection flow of a thermomicropolar fluid past a non-isothermal flat plate". *Int. J. Eng. Sci*. 19 (1981): 1431-1439.

[33] Peddieson, J. "An application of the micropolar model to the calculation of a turbulent shear flow". *Int. J. Eng. Sci*. 10 (1972): 23-32.

[34] Adeniyan, A. "MHD mixed convection of a viscous dissipating and chemically reacting stagnation-point flow near a vertical permeable plate in a porous medium with ther mal radiation and heat source/sink". *Asian Journal of Mathematics and Applications*, (2016): 1-23.

[35] Akinbobola, T. E., Okoya, S. S. "The flow of second grade fluid over a stretching sheet with variable thermal conductivity and viscosity in the presence of heat source/sink". *Journal of Nigeria Mathematical Society*, 34 (2015): 331-342.

[36] Bidin, B., Nazar, R. "Numerical solution of the boundary layer over an exponentially stretching sheet". *European Journal of Scientific Research*, 33 (2009)**:** 710-717.